Sensors & Transducers, Vol. 269, Issue 2, July 2025, pp. 53-61

www.sensorsportal.com

Sensors & Transducers

Published by IFSA Publishing, S. L., 2025
http://www.sensorsportal.com

Extra-long Cooled Organic Substances Phosphorescence Spectra Exciting with Different Radiation Wavelengths

[1,2 *] Dmitry Tsipenyuk, [2] Valery Slobodyanin and [3] Andrey Voropinov

[1] All-Russian Institute of Scientific and Technical Information
of the Russian Academy of Sciences, Usievicha St. 20, Moscow, 125190, Russia
[2] Moscow Institute of Physics and Technology,
Institutsky Pereulok 9, Moscow Region, 141701, Russia
[3] LaserGraphicArt Ltd, Shcherbakovskaya street 53, building 5, Moscow, 105318, Russia
[1] Tel.: +7(499)-152-61-13, fax:+7(499)-943-00-60
E-mail: Dimat777@list.ru, Slobodyanin.v@mail.ru, avv@lasergraphicart.com

Received: 15 April 2025 Revised: 24 June 2025 Accepted:11 July 2025 Published:25 July 2025

Abstract: In this paper, we present an investigation into the dependence of phosphorescence spectra of cooled organic substances on various excitation wavelengths, building on our previous discussions in OPAL'2024 and OPAL'2025 regarding the potential of creating analog optical logical cells in active media cooled to cryogenic temperatures using complex organic compounds. Our findings highlight the feasibility of developing compact optical computing elements based on analogs of the Shpolsky matrix, utilizing a carbon matrix of solid solutions cooled to liquid nitrogen temperature and a monocrystalline $Gd_3Ga_3Al_2O_{12}$:Ce (GAGG:Ce) scintillator-transducer. To advance this technique, it is crucial to understand the physical nature of optical transitions in cooled organic media, which exhibit extra-long visible spectrum phosphorescence lasting up to 5-30 seconds for different substances.

For this purpose, we examined the phosphorescence spectra of various organic substances cooled to cryogenic temperatures under excitation wavelengths ranging from 250-315 nm using UV LEDs, while also investigating the time dependence and magnetic field influence on these spectra. Furthermore, the article explores the potential of creating analog optical computing cells in such cooled active media, integrating organic compounds and scintillating crystals. Phosphorescence was initiated by multiple UV LEDs, each operating independently under distinct electrical signals. Preliminary results of analog summation and integration of optical phosphorescence signals are presented, and the application of this analog process to solving Fourier differential equations is discussed. The possibility of using the investigated composite samples as contact optical sensors for temperature measurements is also considered.

Keywords: Ultralong phosphorescence, Organic molecules, Optical temperature sensors, Cryogenic temperature, Shpolsky, GAGG:Ce transducer, Optical computing.

1. Introduction

Recently, cryoluminescence and triboluminescent-ce have garnered significant attention due to their potential for practical applications [1], such as cryogenic laser creation and the registration of solid object impacts on surfaces [2-5]. Studies have shown that cooling materials enhances both the intensity and duration of luminescence [6-9], a phenomenon observed in various substances, including photonic crystals [10], nanoparticle suspensions, polymers [13, 14], and liquids [15-16]. Luminescence was excited by UV lamp [17, 18] or laser pulses [19, 20]. This paper presents findings on the temporal and spectral characteristics of phosphorescence in organic compounds cooled to liquid nitrogen temperatures. Notably, while some samples lacked luminescence at room temperature or exhibited limited spectral

intervals, all demonstrated prolonged afterglow in the blue-green spectrum under freezing conditions.

These results suggest a common mechanism for long-term luminescence across different organic liquids. Building on our previous research aimed at understanding the physical mechanisms of long-run phosphorescence excitation, we aim to develop an advanced laser based on the Shpolsky matrix analog and explore the potential for creating an optical processor with an extended phosphorescence effect [6, 21-22]. To this end, we examined complex organic materials and various optic and piezo crystals, cocamidopropyl betadine $C_{19}H_{38}N_2O_3$, polyethylene terephthalate $(C_{10}H_8O_4)n$, perfluoro (2-methyl-3-pentanone, Novec 649) $CF_3CF_2C(O)CF(CF_3)_2$, Kalosha benzine (benzine BR-2, Nefras C2 80/120). Different optic and piezo crystals were also investigated: gadolinium aluminum gallium garnet $Gd_3Ga_3Al_2O_{12}$:Ce, lanthanum gallium silicate $La_3Ga_5SiO_{14}$, terbium gallium garnet $Tb_3Ga_5O_{12}$, $La_3Ga_{5,5}Ta_{0,5}O_{14}$.

Solid-state luminescent materials with long lifetimes are increasingly of interest from both scientific and technological perspectives. However, achieving highly efficient organic compounds is often hindered by aggregation-caused quenching and the ultrafast deactivation of excited states [23]. Recent proposals suggest that emission properties in organic molecules can enhanced through the effective stabilization of triplet excited states in H-aggregated molecules, potentially extending luminescence lifetimes to several seconds a significant advancement over conventional organic fluorophores [1]. Our latest research focuses on the temporal and spectral characteristics of phosphorescence in organic compounds cooled to liquid nitrogen temperatures. Luminescence investigations showed that material cooling and other manipulations led to the luminescence intensity and duration increasing [24-28].

While certain organic molecules, such as acetone, ethanol, and isopropanol, exhibit minimal phosphorescence at room temperature, they demonstrate ultralong afterglow in the blue-green spectrum under freezing conditions [5-6, 29-30]. Additionally, we observed that a cooled 77 K opal matrix filled with acetone exhibits both ultralong phosphorescence and X-ray emission with energies exceeding 10 keV under pulsed laser irradiation [31]. These findings prompt us to explore an alternative model, describing extra-long phosphorescence phenomena through the mechanism of electromagnetic field radiation retention by molecules or atoms within an extended space framework [32].

The investigations experimental results could be used for development new optical temperature sensors in the 298-77 K region [33] and optical transducers [34, 35].

Over the past 10 years, there has been an increased interest in developing fluorescent temperature sensors, since these sensors have high measurement accuracy, high sensitivity, as well as fast response and a wide temperature range [36, 37]. It should also be taken into account that the measurement of low (cryogenic) temperatures has unique features. Existing traditional methods of measuring temperatures in the range from 298 to 77 K show low efficiency, which complicates their practical use. Therefore, it is important to study optical temperature measurement, which can realize non-contact measurement of readings, a wide range and fast response. Compounds with an intense luminescence band dependent on temperature can be used as optical materials for such temperature sensors.

2. Experimental Setup

We used two different optical schemes for spectra measurements. First was mercury lamp as an optical pumping source. The radiant power at a wavelength band $\lambda = 230-315$ nm is 24.6 W. The total radiation power is distributed over regions A, B, and C in the following proportions: 21 % in the region A (315–400 nm); 25 % in the region B (280–315 nm); 11 % in the region C (230–280 nm).

The pumping radiation from mercury lamp 1 passing through the focusing quartz collimator 2 and the inverting prism 3 was focused by the quartz lens 4 onto the surface of the investigated sample on a copper cooling line 5 (Fig. 1).

The investigated sample was put onto the surface of a metal cold conductor, partly submerged into liquid nitrogen, which was then poured in the thermostatted cell 6 opened from the top. The time of exposure of the specimens to the pumping radiation was varied in different experimental series from 15 to 60 s. Phosphorescence of specimens 5 through the quartz focusing lens system 7 joined with the quartz optical fiber 8 was registered by a digital spectrum analyzer 9 (manufactured by Ocean Optics) connected with a computer.

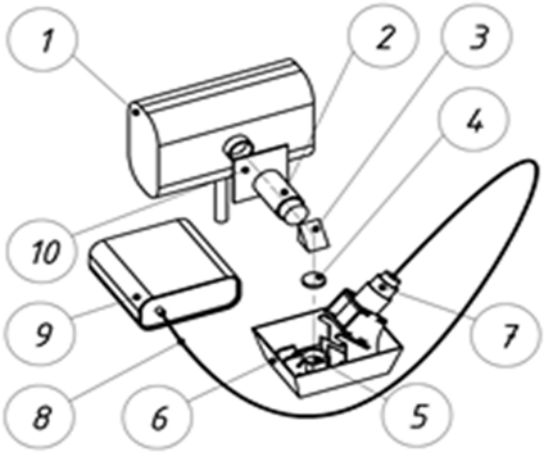

Fig. 1. 1- mercury lamp; 2 - collimator; 3 - inverting prism; 4 - focusing lens; 5 - sample on a copper cooling line; 6 - cell with liquid nitrogen; 7 - collimator; 8 - fiber; 9 spectrometer; 10 replaceable optical filter or mechanical radiation shutter.

The construction of the device provides the possibility of installing replaceable optical filters 10 to extract different bands in the pumping spectrum of the mercury lamp or shutting off the irradiation mechanically. A shutter was used to allow chopping of the incident light to permit measurement of the rise and decay kinetics of the photo-stimulated emission with a time resolution of about 1 msec. To measure the phosphorescence spectra, a cooled specimen was exposed to pumping irradiation for 60 s. After irradiation, the light flux was shut mechanically by an opaque metal gate. The rate of complete shutting of the light pumping flux was measured as 0.1–0.3 s.

At the second optical pumping scheme source, we used different UV LED's (Fig. 2). There were used four types of the UV LED's SMD, which operated in the wave ranges: 255-265 nm, 265-275 nm, 290-300 nm, and 300–315 nm.

A mercury lamp or UV LEDs excited the organic molecules spectra at 77 K, with samples placed on a metal cold conductor partially submerged in liquid nitrogen.

The investigated sample put onto the surface of a metal cold conductor, partly submerged into liquid nitrogen, which poured in the thermostatic cell opened from the top. The time of exposure of the specimens to the pumping radiation was about 20 s. Phosphorescence of specimens through the quartz focusing lens system joined with the quartz optical fiber was registered by a digital spectrum analyzer (manufactured by Ocean Optics) connected with a computer.

A shutter used to allow chopping of the incident light to permit measurement of the rise and decay kinetics of the photo-stimulated emission with a time resolution of about 1.0 msec. Exposure times of the measured phosphorescence spectra were 0.1 s in the presented measurements series.

At Fig. 2, the optical part of the experimental setup with two LEDs is presented.

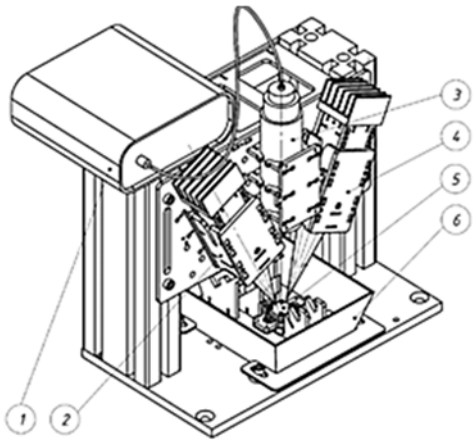

Fig. 2. 1- Spectrometer; 2- UV optical collimator with first diode; 3-quartz collimator for recording phosphorescence coupled with a light guide; 4- UV optical collimator with second diode; 5- organic sample on a metal cooling line cooled up to 77 K; 6- cuvette with liquid nitrogen.

Installations full descriptions were presented in [29, 32].

It should be noted that mercury lamp radiation depends on the lamp design and type (DRT-230 is an arc mercury helium high-pressure quartz lamp). Lamp radiation is variable in time as the mercury lamp heats up during operation [37-38].

Therefore, we controlled the initial radiation spectrum from the DRT-230 when using a mercury lamp as a fluorescence excitation source, in each series of experiments, before and at the end of the measurements. According to the manufacturer's passport data, the DRT-230 lamp power consumption is 230 W, the radiant flux in the range $\lambda = 240–320$ nm is 24.6 W (Fig. 3a and Fig. 3b).

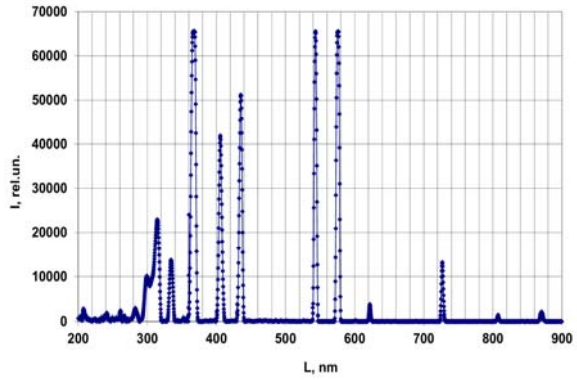

Fig. 3a. Scattered radiation spectrum of a DRT-230 mercury lamp in liquid nitrogen with an empty metal cell 200-900 nm range.

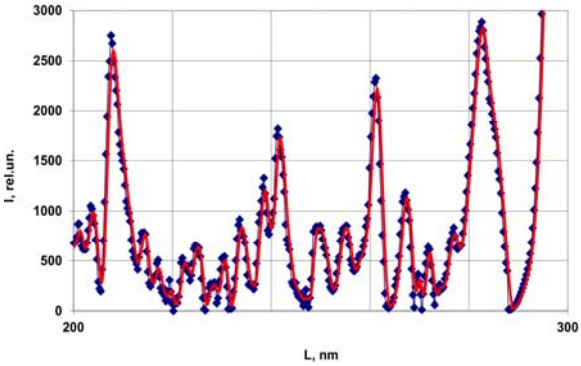

Fig. 3b. Scattered radiation spectrum of a DRT-230 mercury lamp in liquid nitrogen with an empty metal cell 200-300 nm range.

As can be seen from Fig. 3a, and Fig. 3b, emission lines of DRT-230 are located in the areas 207-282, 295-318, 333, 368, 406, 435, 543, 575, 622, 726, 807 and 868 nm. We also took into account the results of studies of the spectral composition and temporal dynamics of radiation from various types of mercury lamps [38, 39]. The measurement technique described above allowed us to control the spectral parameters of the exciting radiation and consistently obtain well-

repeated results of spectral measurements from identical samples in different experimental series.

We investigated samples of the following simple organic molecules: ethanol, isopropanol, acetone, Kalosha benzine, and kokamidopropyl. The freeze-dried samples of nature diamond C_4 and dry ice CO_2 up to 77 K was investigate too.

We illuminated a cooled up to 77 K composed sample (Kalosha benzine and GAGG:Ce scintillate crystal) with different UV LED's. We used UV LED's SMD, which operated in different wave ranges: 255-265 nm, 265-275 nm, 290-300 nm, and 300–315 nm. In Fig. 4, normalized to the maximum spectra of the different UV LED's are presented. The LEDs were driven independently by different electrical signals.

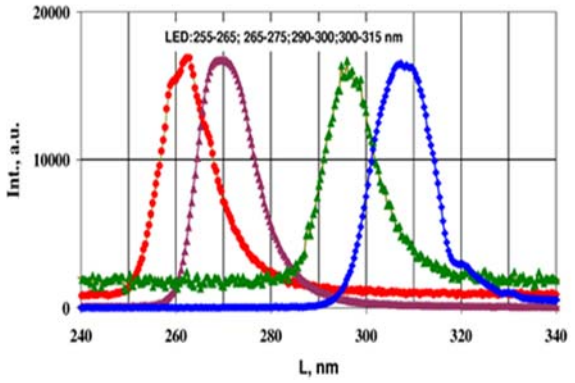

Fig. 4. Normalized UV LED's spectra 255-265, 265-275, 290-300 and 300-315 nm.

Using different LEDs gives us the opportunity to investigate dependence phosphorescence efficiency from the LED's wavelength.

3. Experimental Results

Phosphorescence spectrum of the extra clear ethanol at 77 K. Exposure time 200 ms at the Fig. 5 presented.

Time delay after mercury lamp was switched off is from 200 to 10600 ms.

Note that the liquid sample at room temperature did not glow under similar experimental conditions. Bright luminescence appeared at temperatures close to the temperature of the liquid nitrogen. The intense luminescence had a maximum in the region of 500 nanometers.

The temporal behavior of the extra clear ethanol luminescence is shown in Fig. 6. The phosphorescence lasted about 13 seconds, with the mercury lamp illuminating the sample for 10 seconds. The decay curves demonstrate two-exponential decay behavior without any noticeable build-up stage luminescence in other samples.

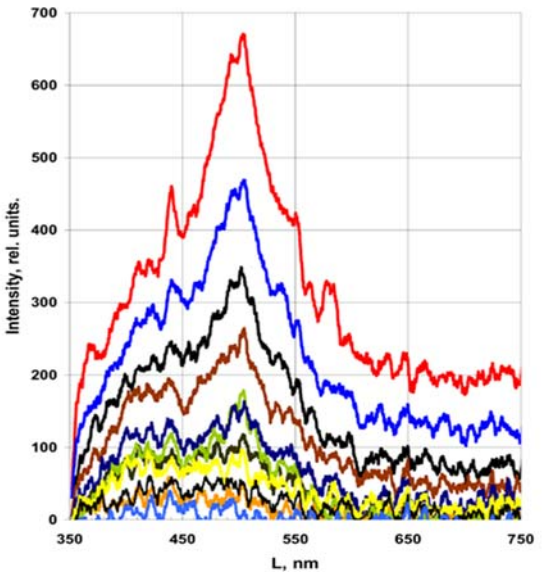

Fig. 5. Phosphorescence spectrum of the ethanol extra clear at 77 K, exposure time 200 ms, time delay after mercury lamp switched off, from the top to the down: 200, 600, 1000, 1800, 2600, 3400, 4600, 6600, 8600, 10600 ms.

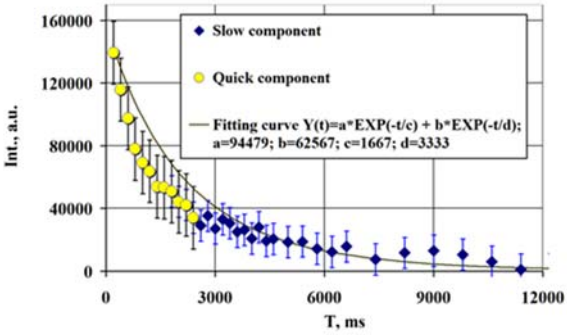

Fig. 6. Temporal extra clear ethanol phosphorescence behavior at 77 K. There are "Slow" and "Quick" components at the exponential fitting curve.

Fig. 7 presents other kinds of our experiments: fluorescence spectrum waveform exited by different light sources investigation (UV LED 255-265, 265-275, and 290-300 nm).

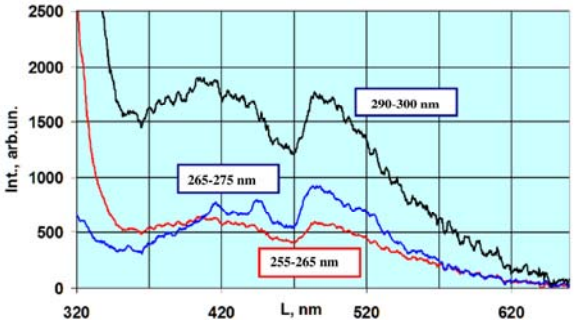

Fig. 7. Ethanol fluorescence, 77 K, integral no delay signal initiated by different UV LEDs: 255-265; 265-275 and 290-300 nm.

At the Fig. 7 there are three ethanol fluorescence spectra. These spectra excited by different diodes. We can find at least one difference in the spectrum waveform (near to 420 and 450 nm) for diode 260-270 nm and two other spectra corresponds to 250-260 and 290-300 nm diodes.

At Fig. 8 Kalosha benzine fluorescence integral signal (no delay) initiated by UV LEDs 255-265 nm at the different sample temperatures 94, 103, and 115 K are presented.

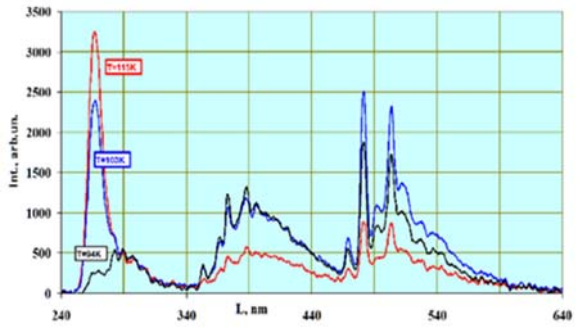

Fig. 8. Kalosha benzine fluorescence integral signal (no delay) initiated by UV LED's 255-265 nm at the different sample temperatures 94, 103 and 115 K.

We can see strong scattered signals from UV LED 255-265 nm at the temperatures 103 and 115 K, but at the 94 K and less UV diode light is mainly absorbed by the cooled organic sample.

In addition, we can find very similar wide luminescence for all temperatures in the 270-320 nm region.

In the region 350-500 nm there is ultralong phosphorescence signal.

The third wideband signal in the region 470-560 nm corresponds to luminescence. It is worth mentioning that all three bands wide signals (270-320, 350-500, and 470-560 nm) have well-defined maximums that give us the possibility to try to elaborate an appropriate optical transition diagram for this case.

Fig. 9 presents result similar to Fig. 8, showing Kalosha benzene fluorescence with no delay at 120 and 136 K using a 255-265 nm UV LED.

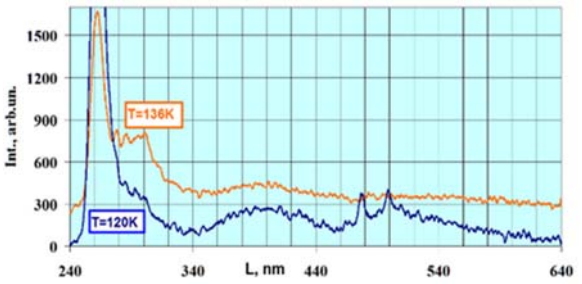

Fig. 9. Kalosha benzine fluorescence integral no delay signal initiated by UV LED 255-265 nm at the different sample temperatures 120 and 136 K.

At the Fig. 8 and Fig. 9 there are a strong scattering signal from the UV LED at 255-265 nm in the spectrum at 103, 115, 120 and 136 K. The amplitude of the degradation spectra decreases, with only two clear peaks at 480 and 500 nm at the 120 K temperature (Fig. 9) and there are no 480 and 500 nm peaks at 136 K.

Once more, in the experimental series, there was luminescence in organic samples under DC magnetic field influence at 77 K (Fig. 10). The DC magnetic field was produced by neodymium magnets and gives us 0.35 T for 2 magnets and 0.44 T for 4 magnets.

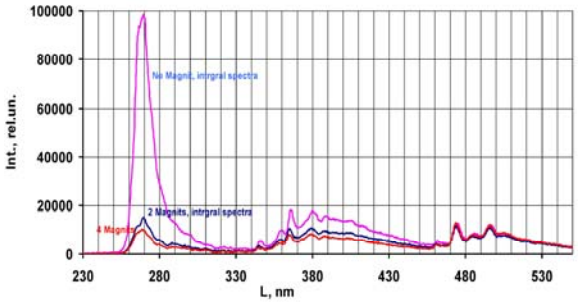

Fig. 10. Kalosha benzine fluorescence integral signal (no delay) initiated by UV LED 265-275 nm at the different DC magnetic field influences at the sample cooled up to 77 K. From the top to the bottom, the magnetic DC field is 0.0 T (no magnets), 0.35 T (2 DC neodymium magnets), and 0.44 T (4 DC neodymium magnets).

As we can see from the Fig. 10 scattered signal from the LED in the region 265-255 nm and phosphorescence in the region 340-450 nm diminished when the magnetic fields increase. At the same time luminescence signal in the region 460-530 nm does not change.

For delayed organic sample spectra under DC magnetic field influence we obtained the same result (Fig. 11).

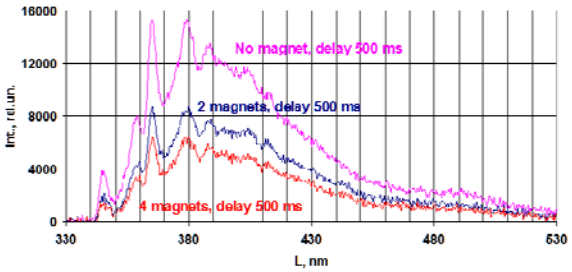

Fig. 11. Kalosha benzine phosphorescence 500 ms delay signal initiated by UV LED 265-275 nm at the different DC magnetic field influences at the sample cooled up to 77 K. From the top to the bottom, the magnetic DC field is 0.0, 0.35 T (2 DC neodymium magnets), and 0.44 T (4 DC neodymium magnets).

We draw attention to the presence of a significant difference in the region of 240-340 nm in the forms of the Kalosha benzine fluorescence integral signals (no

delay) when fluorescence is excited by two different LEDs 255-265 nm (Fig. 8, T=94, 103 and 115 K) and 265-275 nm (Fig. 10, No magnets, 2 and 4 magnets, T=77 K).

We assembled a specially composed sample for the investigation opportunity to use extra-long phosphorescence in analog calculations. We would like to investigate possibility to use this composed sample as contact optical temperature sensor.

The sample consisted of Kalosha gasoline and optical transducer GAGG:Ce cooled to 77 K.

Light from several LED's was used for simulation of fluorescence and phosphorescence spectra in the Kalosha benzine.

The scintillating GAGG:Ce crystal [34, 35] collects light signals from the LEDs and Kalosha benzine and emits a signal that reflects the sum of all.

At the Fig. 12, there are composite samples phosphorescence time dynamics. At the spectra, there are Kalosha gazoline phosphorescence spectra in the region 340-450 nm and initiated by Kalosha benzine phosphorescence, the GAGG:Ce crystal fluorescence spectra in the region 475-670 nm.

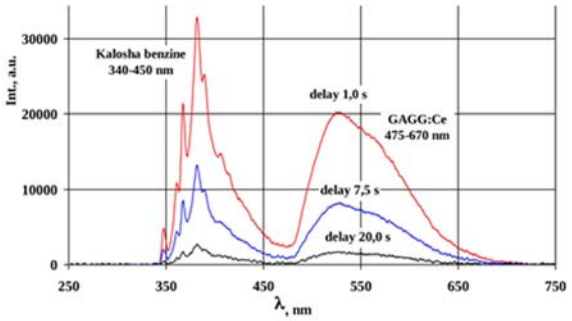

Fig. 12. Time dynamics of composed sample: Kalosha benzine 340-450 nm phosphorescence spectra and GAGG:Ce 475-670 nm crystal fluorescence spectra at 77 K exited by mercury lamp light, exposure time 2.5 s, time delays after the mercury lamp light flux blocking are: 1.0, 7.5 and 20 s (from the top to the bottom).

The spectra Fig. 12 were excited by light from the mercury lamp at 77 K. Complex sample spectra exposure time was 2.5 s, and time delays after the mercury lamp light flux blocking were 1.0, 7.5, and 20 s from the top to the bottom. As we can see from the time dynamics of the composite sample, Kalosha benzine phosphorescence has the same dynamics as the GAGG:Ce crystal fluorescence spectra.

These test experiments show the possibility of using Kalosha benzine plus GAGG:Ce composed sample for optical analog computations such as summarization, integration and differentiation of input optical signals.

For these purposes, we illuminated a cooled up to 77K composed sample (Kalosha benzine and GAGG:Ce scintillate crystal) with different UV LED's. We used UV LED's SMD, which operated in different wave ranges: 255-265 nm, 265-275 nm, 290-300 nm, and 300–315 nm.

At the Fig. 13, we present the first preliminary results of our investigations in analog calculations. This experimental set consists of two LEDs (265-275 and 290-300 nm). Region from A to B both LRD's OFF; from B to C LED 265-275 ON and 290-300 OFF; from C to D both LED's ON; from D to E LED 265-275 ON and 290-300 OFF; from E to F both LED's OFF.

The bottom normalized graph shows the sum of two LEDs light, revealing the dynamics of changes in optical excitation signal from two LEDs. The total time of the experiment was 80 seconds, and the and the time of exposure for each point was 0.2 s.

The middle graph in Fig. 13 shows the normalized average optical signal in the range of 385-395 nm from Galosh gasoline. As you can see in the range B - C the signal increases according to the logarithmic law, and decreases in the range E - F according to the exponential law. Section B-C corresponds to the accumulation of a signal from ultra-long-term phosphorescence when excited by a 265-275 nm LED, and Section E-F corresponds to a gradual decrease in the phosphorescence signal in the complete absence of optical pumping.

In Section C-D, we studied the change in response in Galosh gasoline when another LED 290-300 nm was turned on/off. It can be seen that at point C, the signal increases sharply and decreases sharply at point D when the LED 290-300 nm turns off. This difference in the time dynamics of the increase and decrease of the optical signal from Kalosh gasoline is due to different lifetimes of excited states when irradiated in different wavelength ranges 265-275 versus 290-300 nm.

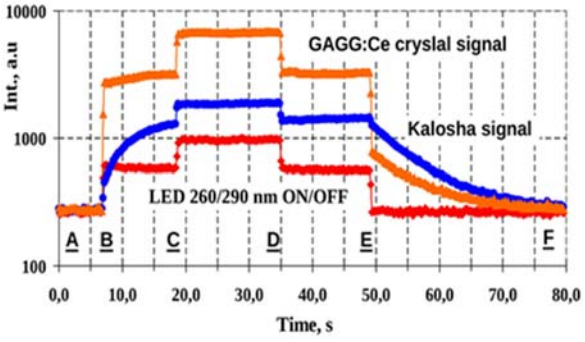

Fig. 13. Composed of three datasets from optical signals left to right: A to B LED's 265 and 290 are OFF; B to C LED's 265 is ON and 290 nm is OFF; C to D LED's 265 and 290 nm are ON; D to E LED's 265nm and 290nm are off; and E to F LED's 265 and 290nm are off. From the bottom to the top: optical signals from two LEDs 265 and 290 nm (mean value 26-300 nm); Kalosha benzine fluorescence signal (mean value 385-395 nm); GAGG:Ce scintillator (mean value 530-540 nm).

As a result of the experiments, we were able to compare the speed and efficiency of excitation of

optical responses in the sample under study when excited from light sources of different wavelengths.

The top graph of Fig. 13 shows the response (average optical response in the range 530-540 nm) of a single crystal scintillator to the total optical signal excited by LEDs in a sample of Galosh gasoline frozen to 77 K.

We estimate the efficiency of excitation of the optical signal in the scintillator to be very high. For example, Fig. 12 shows that the total area under the phosphorescence signal of Kalosh gasoline (range 350-450 nm) and the optical response of the scintillator (range 475-670 nm) are equal.

We consider the results of testing an optical complex sample with excitation of fluorescence and phosphorescence in the sample by controlled signals to be promising for the creation of an optical analog memristor using this technology.

It is possible to try to use this Kalosha benzine and optical transducer GAGG:Ce composed sample as a contact optical temperature sensor [6, 36-37].

4. Conclusions

The idea to investigate different organic materials cooled up to the 77 K phosphorescence has a relatively long history.

At the beginning [31] we investigated luminescence properties of the photonic crystals (synthetic opal matrices SiO_2 with voids, infiltrated with ethanol or acetone) under the influence of a single ruby laser pulse (10 ns, 694.3 nm) focused mode at 77 K.

During more experiments, we found that focused single pulse laser and photonic crystals are not necessary for extra-long phosphorescence initiation.

Phosphorescence pumping occurs in any organic samples in a threshold-free manner by continuous radiation with a pump radiation length shorter than 300 nm and cooling of the sample to a temperature of 77 K [5-6, 29].

Our experimental studies have shown the absence of any significant phosphorescence in the 300-700 nm region in pure water (H2O), pure carbon (natural diamonds C4), dry ice (CO2), liquid nitrogen (N2) when cooling samples to a temperature of 77K and irradiating with pulsed or continuous radiation shorter than 300 nm.

Today we focused on studying the ultra-long phosphorescence of the following organic compound samples: ethanol, isopropanol, and Kalosha benzine.

The choice determined by the following considerations: ethanol and isopropanol are among the simplest and most thoroughly studied organic substances; isopropanol and Kalosha benzine have shown the greatest efficiency in converting exciting radiation into ultra-long phosphorescence.

The experimental setup using UV LEDs covering different wavelength ranges (255–265 nm,

265–275 nm, 290–300 nm, and 300–315 nm) allows us to study in detail how different parts of the UV excitation spectrum in the range of 250–320 nm excite phosphorescence in the studied samples. In the previous studies, a mercury lamp or a continuous spectrum of plasma arising from the breakdown of a focused pulsed laser radiation served as the excitation source [5-6, 9, 29].

The studies performed using different LEDs confirmed our earlier conclusion that ultralong phosphorescence is initiated in cooled organic samples in a threshold-free manner under the influence of radiation shorter than 300 nm. In addition, the use of UV sources of different wavelengths allows us to obtain experimental data for constructing a model of ultra long phosphorescence [22].

As the conducted experimental studies have shown, temperature-dependent changes in phosphorescence signals are especially significant.

In our opinion, the fundamental physical mechanisms that explain these changes at different temperatures may consist of an increase in the mobility of molecules with increasing temperature, which leads to the depletion of triplet levels, or perhaps there is an optical trap phenomenon, where the non-uniform distribution of the electromagnetic field forms an effective potential well for particles.

Regarding the experimental reproducibility of the obtained results, we found that with different settings or minor changes in the composition of the organic samples, different results could be obtained.

For example, the study of phosphorescence of ethanol of different origins and purity gave phosphorescence spectra that differed significantly from each other. We plan to devote a separate study to this result.

To explain the effect of super long phosphorescence of organic substances, it is possible to apply different approaches and models. In particular, a number of recent experimental studies of phosphorescence of complex organic compounds have shown the presence of long-term phosphorescence in the studied samples [1-3, 14-20, 23-28]. The experimental results presented in the papers confirmed by model calculations. The samples of organic compounds that we study are much simpler in composition.

We do not know of any triplet levels in the ethanol that can give us super long phosphorescence in the visible region. From our point of view, presented experiments could give us possibilities to elaborate an optical transitions model well described by ultra long phosphorescence for simple organic molecules cooled up to 77 K.

From our point of view, presented experiments could give us possibilities to elaborate an optical transitions model well described by ultra long phosphorescence for simple organic molecules cooled up to 77 K.

As one of the possible models, we would like to consider approaches developed in [32] for the electromagnetic field in the extended 5-dimensional space model, its localization, and its interaction. Such model could leads to the photon with mass in the

external field and as a result could build physical phenomenological model with an optical trap phenomenon.

For this reason, we are also considering other, more exotic models to explain this effect. We wish to take into account the ideas concerning linked and knotted beams of light [40-42] and limits on electrodynamics developed in [43].

We would like to attract your attention that some other science groups involve exotic model "quantum-entangled electronically excited states" for description experimental results in the organic molecules samples (naphthalene) [44] "An experiment is proposed that can confirm the existence and possibility of realization of quantum-entangled electron-excited states of hydrocarbon molecules" also.

Acknowledgements

Authors would like to reveal thanks Shenzhen Trillion Auspicious Lighting Co., Ltd. for the cooperation in supply with necessary LED SMD 20 mm Copper PCB samples.

The authors also are thankful for the Oleg A Buzanov and OJSC «Fomos Materials» for the crystals sample investigated in the paper.

References

[1]. Z. An, C. Zheng, Y. Tao, R. Chen, H. Shi, T. Chen, Z. Wang, H. Li, R. Deng, X. Liu, W. Huang, Stabilizing triplet excited states for ultralong organic phosphorescence, *Nature Materials*, Vol. 14, Issue 7, 2015, pp. 685–690.

[2]. K. K. Contag, M. Karszewski, et al., Theoretical modelling and experimental investigations of the diode-pumped thin-disk Yb:YAG laser, *Quantum Electronics*, Vol. 29, Issue 8, 1999, pp. 697–703.

[3]. T. Y. Fan, et al., Cryogenic Yb^{3+}-doped solid-state lasers, *IEEE Journal of Selected Topics in Quantum Electronics*, Vol. 13, Issue 3, 2007, pp. 448–459.

[4]. A. Soloviev, et al., Experimental study of thermal lens features in laser ceramics, *Optics Express*, Vol. 16, Issue 25, 2008, pp. 21012–21021.

[5]. A. V. Voropinov, et al., Long-term luminescence in organic liquids at low temperatures, *Laser Physics Letters*, Vol. 18, Issue 7, 2021, pp. 148–152.

[6]. Yu. K. Aleshin, et al., Development of a laser generator based on the analog of the Shpol'sky matrix, *Moscow University Physics Bulletin*, Vol. 74, 2019, pp. 52–56.

[7]. V. S. Gorelik, et al., Spectral characteristics of the radiation of artificial opal crystals in the presence of the photonic flame effect, *JETP Letters*, Vol. 84, Issue 9, 2007, pp. 485–489.

[8]. N. V. Chernega, A. D. Kudryavtseva, Nonlinear-optical properties of photonic crystals, *Journal of Surface Investigation: X-ray, Synchrotron and Neutron Techniques*, Vol. 3, Issue 4, 2009, pp. 513–518.

[9]. A. V. Voropinov, D. Y. Tsipenyuk, in *Proceedings of the XXIX International Conference 'Lasers in Science, Technology, and Medicine'*, Moscow, Russia, 2018, p. 93.

[10]. M. V. Vasnetsov, V. Y. Bazhenov, Luminescence response of synthetic opal under femtosecond laser pumping, *Journal of Luminescence*, Vol. 166, 2015, pp. 233–237.

[11]. H. Ehrlich, A. Kudryavtseva, G. Lisichkin, V. Savranskii, N. Tcherniega, et al., Frozen ZnS aqueous suspension nonlinear optical properties, *International Journal of Thermophysics*, Vol. 36, Issues 10–11, 2015, pp. 2784–2791.

[12]. A. Anjiki, T. Uchino, Visible photoluminescence from photoinduced molecular species in nanometer-sized oxides: crystalline Al_2O_3 and amorphous SiO_2 nanoparticles, *The Journal of Physical Chemistry C*, Vol. 116, Issue 29, 2012, pp. 15747–15755.

[13]. N. A. Bulychev, M. A. Kazaryan, A. D. Kudryavtseva, M. V. Kuznetsova, et al., Anti-Stokes luminescence in nanoscale systems, in *Proceedings of SPIE, International Conference on Atomic and Molecular Pulsed Lasers XIII*, Vol. 10614, 2018, Article 106140N.

[14]. M. E. Kompan, I. G. Aksyanov, Near-UV narrow-band luminescence of polyethylene and polytetrafluoroethylene, *The Physics and Engineering of Solid State Lasers*, Vol. 51, 2009, pp. 1083–1086.

[15]. G. J. Minkoff, Frozen Free Radicals*, Interscience Publishers Inc.,* New York, 1960.

[16]. D. L. Kirko, Luminescence of liquid nitrogen after exposure to pulsed UV radiation, *Low Temperature Physics*, Vol. 41, 2015, pp. 303–307.

[17]. D. Denzler, et al., Luminescence studies of localized gap states in colloidal ZnS nanocrystals, *Journal of Applied Physics*, Vol. 84, 1998, pp. 2841–2485.

[18]. K. Kimura, Blue luminescence from silicon nanoparticles suspended in organic liquids, *Journal of Cluster Science*, Vol. 10, 1999, pp. 359–380.

[19]. Y. D. Glinka, et al., Size effect in self-trapped exciton photoluminescence from SiO_2-based nanoscale materials, *Physical Review B*, Vol. 64, 2001, Article 085421.

[20]. Z. Li, H. Meng, Organic Light-Emitting Materials and Devices*, CRC Press*, Boca Raton, FL, 2017.

[21]. D. Y. Tsipenyuk, V. P. Slobodyanin, et al., Extra long phosphorescence in organic materials at cryogenic temperatures investigation, *Laser Physics Letters*, Vol. 20, 2023, Article 126002.

[22]. D. Yu. Tsipenyuk, V. P. Slobodyanin, A. V. Voropinov, Possibility to use long-term phosphorescence of the cooled organic substances for analog optical computing, in *Proceedings of the 7th International Conference on Optics, Photonics and Lasers (OPAL' 2024)*, 15–17 May 2024, Palma de Mallorca (Balearic Islands), Spain, 2024, pp. 70–75.

[23]. E. Lucenti, A. Forni, C. Botta, et al., Phosphorescence from a pure organic molecule, *The Journal of Physical Chemistry Letters*, Vol. 8, Issue 8, 2017, pp. 1894–1898.

[24]. Z. Ma, Z. Yang, L. Mu, et al., Converting molecular luminescence to ultralong room-temperature phosphorescence via the excited state modulation of sulfone-containing heteroaromatics, *Chemical Science*, Vol. 12, Issue 44, 2021, pp. 14808–14814.

[25]. G. Bao, R. Deng, D. Jin, X. Liu, Hidden triplet states at hybrid organic–inorganic interfaces, *Nature Reviews Materials*, Vol. 9, 2024, pp. 1–14.

[26]. B. Madushani, M. Mamada, K. Goushi, et al., Multiple donor–acceptor design for highly luminescent and stable thermally activated delayed fluorescence emitters, *Scientific Reports*, Vol. 13, Issue 1, 2023, Article 7644.

[27]. J. Choi, H. Im, J. M. Heo, D. W. Kim, et al., Microsecond triplet emission from organic chromophore–transition metal dichalcogenide hybrids via through-space spin orbit proximity effect, *Nature Communications*, Vol. 15, 2024, Article 10282.

[28]. L. Hua, Y. Liu, B. Liu, Z. Zhao, et al., Constructing high-efficiency orange-red thermally activated delayed fluorescence emitters by three-dimension molecular engineering, *Nature Communications*, Vol. 13, 2022, Article 7828.

[29]. Y. K. Aleshin, D. Yu. Tsipenyuk, A. V. Voropinov, The time characteristics and phosphorescence spectra of cooled carbon-containing analogues of the Shpolsky matrix, *Moscow University Physics Bulletin*, Vol. 75, 2020, pp. 148–152.

[30]. D. Yu. Tsipenyuk, V. P. Slobodyanin, A. V. Voropinov, Cooled organic substances long-term phosphorescence spectra dependence from exciting radiation wavelength, in *Proceedings of the 8th International Conference on Optics, Photonics and Lasers (OPAL' 2025)*, 14–16 May 2025, Rhodes, Greece, 2025, pp. 99–102.

[31]. N. V. Cherniega, A. A. Kraiskii, A. V. Kraiskii, D. Yu. Tsipenyuk, Generation of narrowly directed X-rays under optical pumping in synthetic opal matrices, *Bulletin of the Lebedev Physics Institute*, Vol. 37, 2010, pp. 89–94.

[32]. V. A. Andreev, D. Yu. Tsipenyuk, Electromagnetic field in the extended space 5-dimensional model, its localization and interaction with waveguide, *RENSIT: Radioelectronics. Nanosystems. Information Technologies*, Vol. 11, Issue 2, 2019, pp. 93–102.

[33]. E. N. Bocharnikova, I. A. Konov, A. E. Kurtsevich, I. V. Aksenova, New optical materials for cryogenic temperature sensor based on bis(dipyrromethene) complexes, *Izvestiya vuzov. Fizika*, Vol. 66, Issue 10, 2023, pp. 5–16. (in Russian)

[34]. N. S. Kozlova, O. A. Buzanov, V. M. Kasimova, A. P. Kozlova, E. V. Zabelina, Optical characteristics of single crystal $Gd_3Al_2Ga_3O_{12}$:Ce, *Modern Electronic Materials*, Vol. 4, 2018, pp. 7–12.

[35]. K. Kamada, T. Yanagida, T. Endo, K. Tsutumi, Y. Usuki, M. Nikl, 2-inch size single crystal growth and scintillation properties of new scintillator Ce:$Gd_3Al_2Ga_3O_{12}$, in *Proceedings in the IEEE Nuclear Science Symposium and Medical Imaging Conference (NSS/MIC' 2011)*, Valencia, Spain, 2011, pp. 1927–1929.

[36]. X. D. Wang, O. S. Wolfbeis, R. J. Meier, Luminescent probes and sensors for temperature, *Chemical Society Reviews*, Vol. 42, 2013, pp. 7834–7869.

[37]. Yan Zhao, Xusheng Wang, Ying Zhang, Yanxia Li, Xi Yao, Optical temperature sensing of up-conversion luminescent materials: Fundamentals and progress, *Journal of Alloys and Compounds*, Vol. 817, 2020, Article 152691.

[38]. I. Konyushenko, Hamamatsu Mini MS Series spectrometers, *Components & Technologies*, Vol. 2, 2012. Available at: https://kit-e.ru/mini-spektrometry-serii-ms-firmy-hamamatsu/

[39]. E. V. Avramenko, A. V. Khabarova, A. S. Sherstobitova, et al., Time dynamics of the radiation spectrum of the DRGS-12 mercury-helium lamp, *Measurement Techniques*, Vol. 58, 2015, pp. 300–302.

[40]. W. T. M. Irvine, D. Bouwmeester, Linked and knotted beams of light, *Nature Physics*, Vol. 4, 2008, pp. 716–720.

[41]. H. K. Moffatt, The degree of knottedness of tangled vortex lines, *Journal of Fluid Mechanics*, Vol. 35, Issue 1, 1969, pp. 117–129.

[42]. N. Wolchover, Mysteries of fluid flow unraveled by knots, *Scientific American*, 2023. Available at: https://www.scientificamerican.com/article/mysteries-of-fluid-flow-knots/

[43]. L. B. Okun, Limits on electrodynamics: paraphotons?, *Zhurnal Éksperimental'noĭ i Teoreticheskoĭ Fiziki*, Vol. 83, 1982, pp. 892–898. (in Russian)

[44]. G. V. Mayer, O. N. Tchaikovskaya, O. K. Bazyl, E. N. Bocharnikova, The physical manifestation of quantum-entangled electronically excited states in polyatomic molecules, *Izvestiya vuzov. Fizika*, Vol. 68, Issue 2, 2025, pp. 5–10. (in Russian)

Published by International Frequency Sensor Association (IFSA) Publishing, S. L., 2025 (http://www.sensorsportal.com).